Contents lists available at ScienceDirect

Journal of Atmospheric and Solar-Terrestrial Physics

journal homepage: www.elsevier.com/locate/jastp

Comparative study of lightning climatology and the role of meteorological parameters over the Himalayan region

Narayan Prasad Damase [a], Trisanu Banik [c], Bapan Paul [b], Kumarjit Saha [b], Shriram Sharma [d], Barin Kumar De [b], Anirban Guha [b,e,*]

[a] District Administration Office, Arghakhanchi, Nepal
[b] Department of Physics, Tripura University, Tripura, 799022, India
[c] North Eastern Space Applications Centre, Umiam, 793103, Meghalaya, India
[d] Department of Physics, Amrit Science College, Tribhuvan University, Kathmandu, Nepal
[e] Center for Lightning and Thunderstorm Studies, Department of Physics, Tripura University, Tripura, 799022, India

ARTICLE INFO

Keywords:
Lightning imaging sensor
Himalayan lightning
Relative humidity

ABSTRACT

Lightning activities are distributed asymmetrically over the globe. Satellite images show that the Himalayan region is one of the prone zones of lightning activity. We do not understand such an uneven distribution of lightning activities as of today. To elaborate on the present-day understanding of lightning flashes over the Himalayan region, we have analyzed various atmospheric factors in association with Lightning Flash Density (LFD). For this purpose, we divided the Himalayan Range into three sections, namely, eastern, middle, and the western Himalayas. We explored the possible association of monthly mean Convective Available Potential Energy (CAPE), Surface Air Temperature (SAT), thermodynamic temperature of the top of the cloud; Cloud Top Temperature (CTT), Relative Humidity (RH), and Specific Humidity (SH) with LFD over the three sections of the Himalayan range. We observed that CAPE and SAT play a vital role in creating instability over that region. In contrast, moderate moisture (i.e., RH) is the most suitable condition for lightning activities over all three sections. The analysis shows that 50–60% RH at 700hpa is the most favorable condition for lightning over the Himalayan region.

1. Introduction

Satellite images of lightning activities show that the Himalayan region is one of the world's lightning prone areas (https://ghrc.nsstc.nasa.gov/lightning/data/data_lis_trmm.html). Due to the topology, varied surface temperature, moisture, and atmospheric circulation, lightning flash density (LFD) over this region have a tremendous spatiotemporal variability. From the pre-South-East monsoon study during 2012 over Nepal, we observe the peak in the lightning flash count (LFC) to be maximum in June (Makela et al., 2014). The variation of lightning activity over the Northeastern part of the Himalayan region is semiannual with primary maxima during April. But the similar maxima occurs during July in the North-West region (Penki and Kamra, 2013). The fundamental reason behind this variation of lightning activity was an unanswered question. In this paper, we analyzed the role of moisture (in terms of relative humidity) and other meteorological parameters on lightning activity and also explained the significant influence of RH over the lightning generation process.

The scientific community has proposed several theories of the cloud electrification mechanism and separation of charges within the clouds. However, the most significant cloud electrification approach is the graupel-ice mechanism. Collisions produce electric charges between precipitation particles (graupel) and cloud particles or small ice crystals (Rakov and Uman, 2003; Hobbs and Burrows, 1966; Takahashi, 1978; Saunders and Peck, 1998). The action of gravity is mainly responsible for separating the charged particles (Rakov and Uman, 2003). The significant impact of CAPE on LFD recently been observed by Qie et al. (2020). The decrease of the CAPE could exert the most considerable effect on decreasing the LFD trend on Southern North America (SENA), Central South America (CSA), and Eastern Australia (EA) (Qie et al., 2020). Dewan et al. (2018) observed the influence of CAPE impact the lightning activity positively. It is a well established fact that Convective Available Potential Energy, creates instability in the atmosphere, causes updrafts and supports electrification and charge separation within the

* Corresponding author. Department of Physics, Tripura University, Tripura, 799022, India.
E-mail address: anirban1001@yahoo.com (A. Guha).

https://doi.org/10.1016/j.jastp.2020.105527
Received 12 April 2020; Received in revised form 14 December 2020; Accepted 17 December 2020

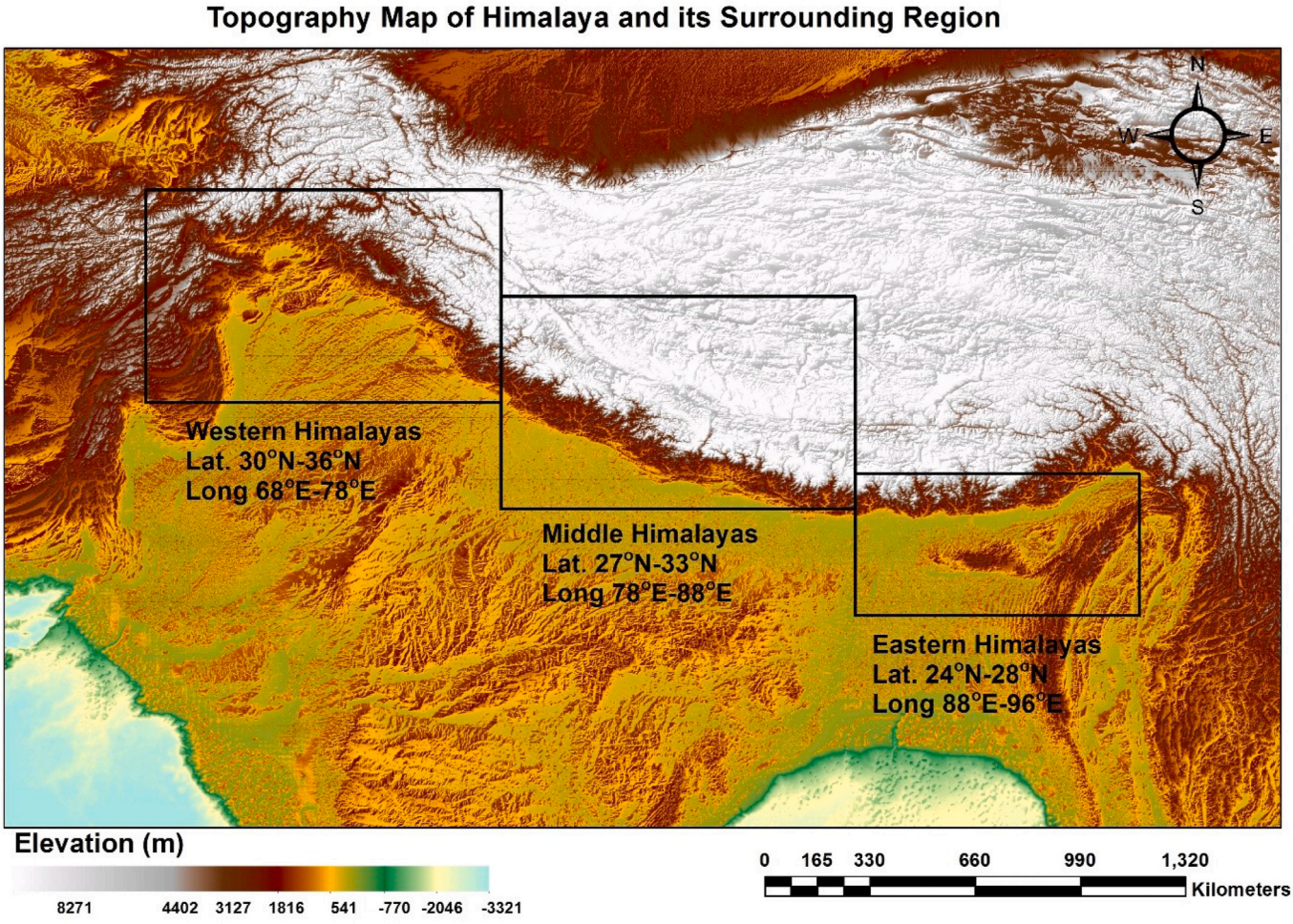

a

Fig. 1. a: Topography map of the Himalayas and its surrounding regions. b: Density plot of lightning activity over the Himalayan region from 1998 to 2013. The Eastern Himalayas, Middle Himalayas and Western Himalayas are represented by the rectangles. The numbers in the top right corner represents the months (1-January, 2-February etc.). c: The time-averaged map of Normalized Difference Vegetation Index (NDVI) from 2000 to 2013. d: Time averaged map of precipitation from 1998 to 2013.

clouds. A good relationships with total lightning activity ($r = 0.93$) was observed if updraft volume in the charging zone (at temperatures colder than -5^0C) with vertical velocities greater than either 5 or 10 m/s (Deierling and Petersen,2008). High lightning activity is related to CAPE's high value over Greece (Mazarakis et al., 2008). A high correlation of lightning flashes and CAPE over Maharashtra, India has been observed by Tinmaker et al. (2015); whereas, the relationship between LFC and CAPE has not been observed consistent in different regions of India (Siingh et al., 2014). Zheng et al. (2016) studied the sensitivity of lightning with CAPE and showed that lightning is more sensitive to CAPE over land than offshore water. A good correlation coefficient between LFC with CAPE and surface temperature over Northeast India was observed by Guha et al. (2017).

Pinto and Pinto (2008) studied the sensitivity of lightning cloud-to-ground (CG) activity with the surface air temperature daily, monthly, yearly, and decadal time scale. Pinto and Pinto (2008) found a sensitivity of 40% per 1^0C at daily and monthly timescales and 30% sensitivity per 1^0C at decadal timescales. The lightning sensitivity of the order of 10% per 1^0C has been observed by Williams (1994) that further supports the positive correlation between lightning activity and surface temperature for the annual and semiannual timescale. Ming et al. (2005) and Saha et al. (2019) derived the positive response of the surface air temperature (SAT) on the lightning flash rate for inter-annual and seasonal timelines. In the monthly time scale, from May to September via pre-monsoon cooling of 1^0C in maximum SAT reduces approximately 3.5 thunderstorms per station and 73 flashes (Nath et al., 2009). The correlation between change in global monthly land wet-bulb temperature with lightning activity is strongest over the northern hemisphere and weak in the southern hemisphere (Reeve and Toumi, 1999). A 1^0C rise in temperature increases 20–44% lightning flash density over the land mass Indian region (Kandalgaonkar et al., 2005).

For years, the effect of relative humidity (RH) on lightning became one of the burning issues in atmospheric electricity research. Ya-Jun et al. (2006) have observed that higher RH results in more lightning activity in dry regions, whereas less lightning activity in wet areas. Reeve and Toumi (1999) indicate the necessity of a high land-area to sea-area ratio for a good correlation between lightning activity and land wet-bulb temperature. But the complete understanding of the effect of

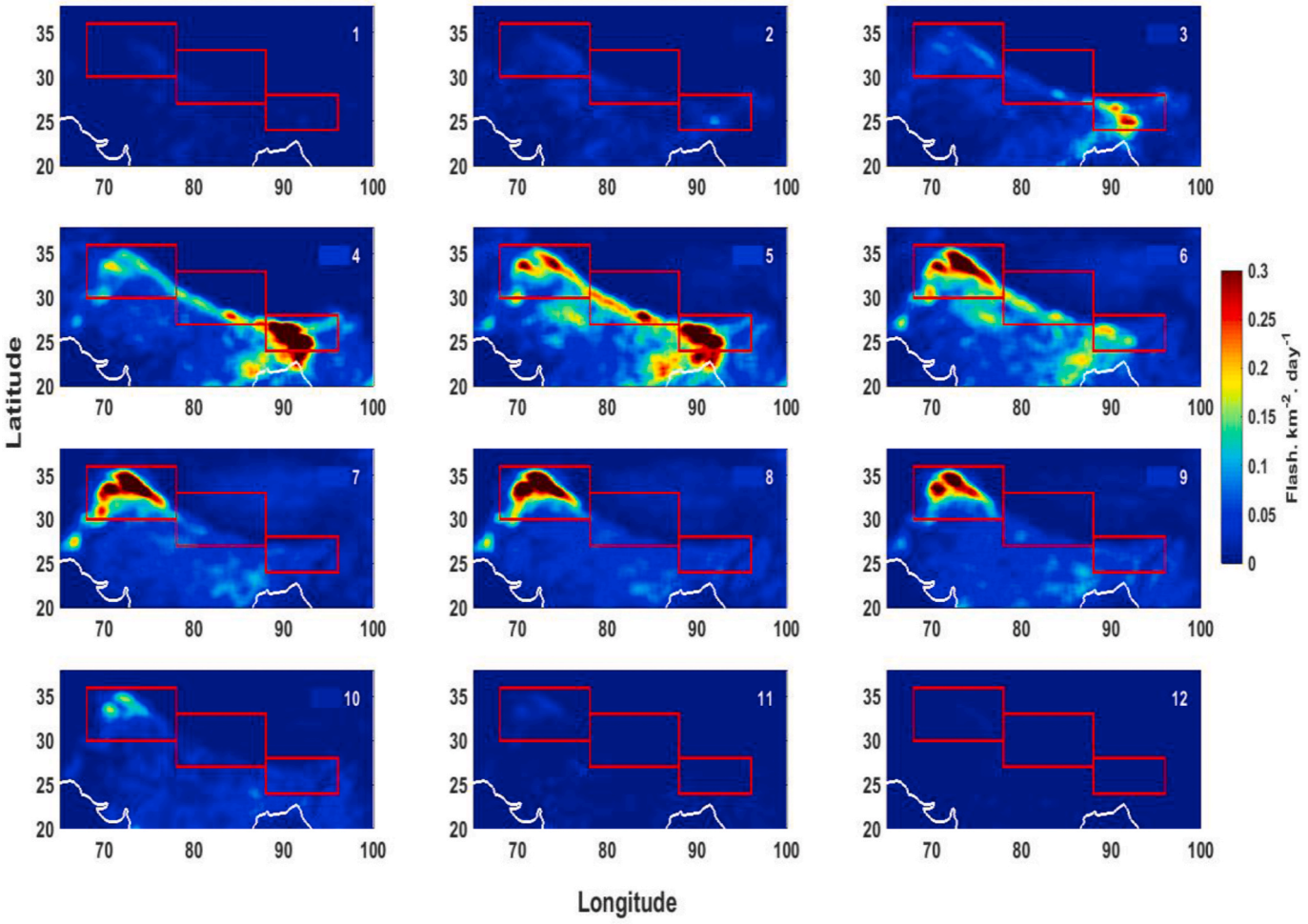

b

Fig. 1. (*continued*).

RH on lightning is still lacking. The role of cloud base height and associated cloud top temperature on the lightning flash is critical in this regard. Molinie and Jacobson (2004) show an increase of lightning flash density with a decrease in cloud top brightness temperature (CTBT); the temperature of a black body that would emit the same amount of radiation as the targeted body in a specified spectral band when CTBT is less than -55^0C. An intense condensation process and mass flux during the system's growth phase can provide favorable cloud electrification conditions and lightning (Mattos and Machado, 2011).

In the present research, we have analyzed the role of CAPE, SAT, RH, CTT, and precipitation on lightning activity in different parts of the Himalayas. We selected the regions of investigation as the Eastern Himalayas (24^0N–28^0N, 88^0E-96^0E), the middle Himalayas (27^0N–33^0N, 78^0E-88^0E), and the Western Himalayas (30^0N–36^0N, 68^0 E–78^0E). We describe the study region and its topology in Fig. 1a. The lightning density map, NDVI index map, and precipitation map are illustrated in Fig. 1b, 1c, and 1d, respectively. The middle Himalayas contains high hills and mountains followed by Western Himalayas, and the Eastern Himalayas has the least elevation.

2. Data

We used Tropical Rainfall Measuring Mission (TRMM) Lightning Imaging Sensor (LIS) observation 0.1° very high-resolution gridded lightning monthly climatology (VHRMC) data to compute the seasonal variation of lightning density over the Himalayan region. LIS is a space-based instrument onboard the Tropical Rainfall Measurement Mission (TRMM) satellite to observe the distribution and variability of total lightning (cloud-to-cloud, intra-cloud, and cloud-to-ground lightning) within the tropical belt of the Earth. It can detect lightning flashes with 93±4% efficiency during nighttime and 73±11% efficiency during daytime (Boccippio et al., 2002). It locates lightning flashes with 4-7 km spatial resolution and temporal resolution of 2 ms, over a vast region of Earth surface along the orbital track of the satellite (Siingh et al., 2014). Orbital track lightning flashes are used to find the effect of other meteorological parameters like CAPE (NCEP/NCAR reanalysis of size grid 180 × 91 × 1704, dimension lon, lat, time), SAT (Meera 2 model with monthly temporal resolution and 0.5 × 0.625° spatial resolution), RH at 700 hPa and SH at 950 hPa (Meera model with monthly temporal resolution and 1.25° spatial resolution), CTT (Meera model with monthly temporal resolution and 0.5 × 0.667° spatial resolution), Aerosol Optical Thickness 550 nm (AOT) (Meera 2 model with monthly temporal resolution and 0.5 × 0.625° spatial resolution). Also, monthly values of 2.5-degree latitude × 2.5-degree longitude of global grid (144 × 72) CPC merged analysis of precipitation (CMAP), monthly mean 2.5-degree latitude × 2.5-degree longitude of global grid (144 × 73) NCEP/NCAR reanalysis wind speed are used for the study. The topology data used here is from ETOPO1 datasets, which has the resolution of 1 arc-minute (around 1.7 km) globally and represents the Earth's topography and ocean bathymetry. This is the initiative of NOAA-NCEI

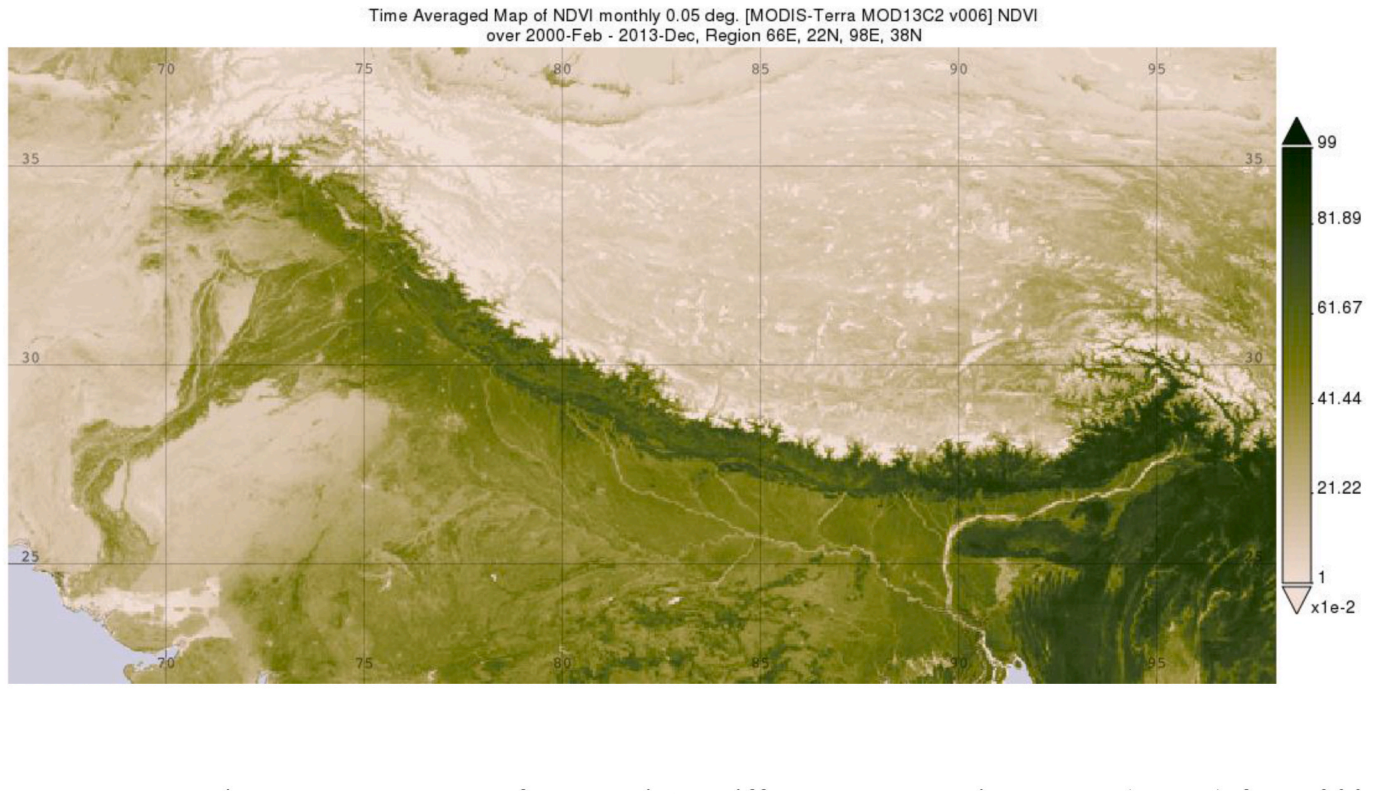

c

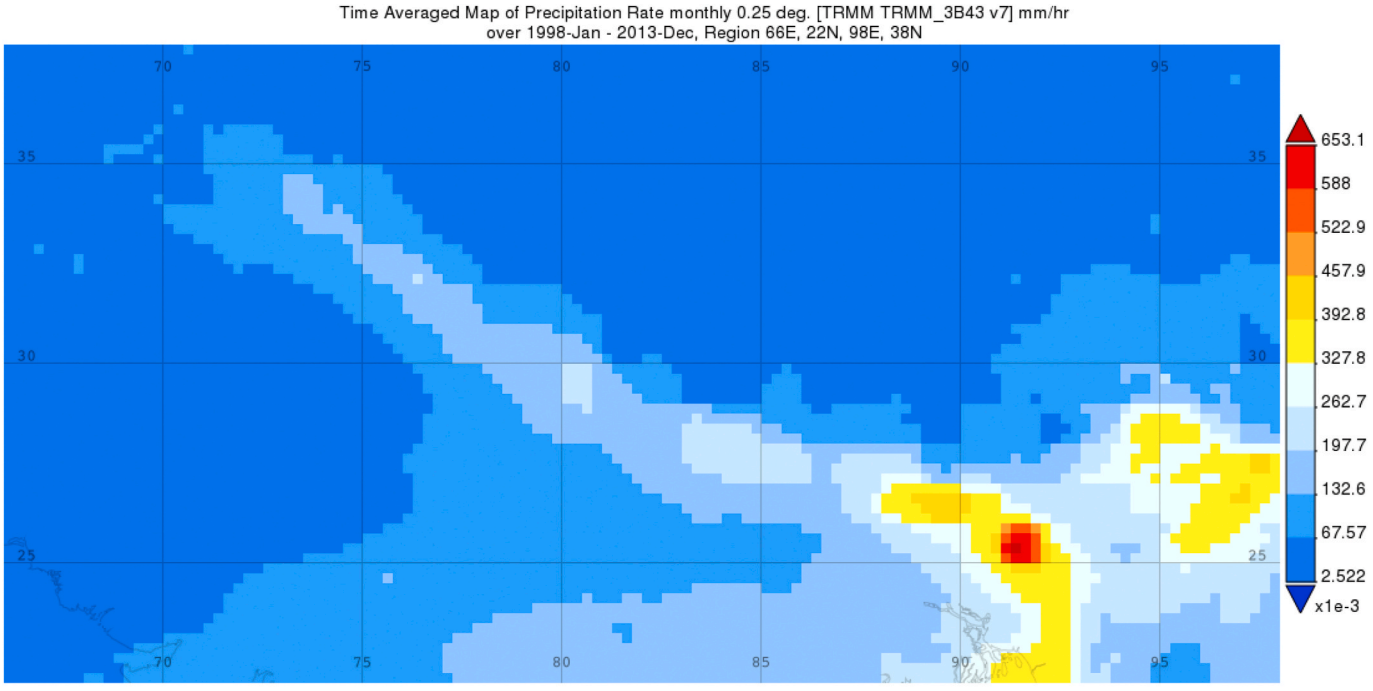

d

Fig. 1. (*continued*).

(National Centers for Environmental Information) data center; they collected global and regional datasets together to build the ETOPO1 database.

3. Methodology

In the present study for the comparative analysis, lightning flashes detected by LIS are used. To find the influence of others meteorological

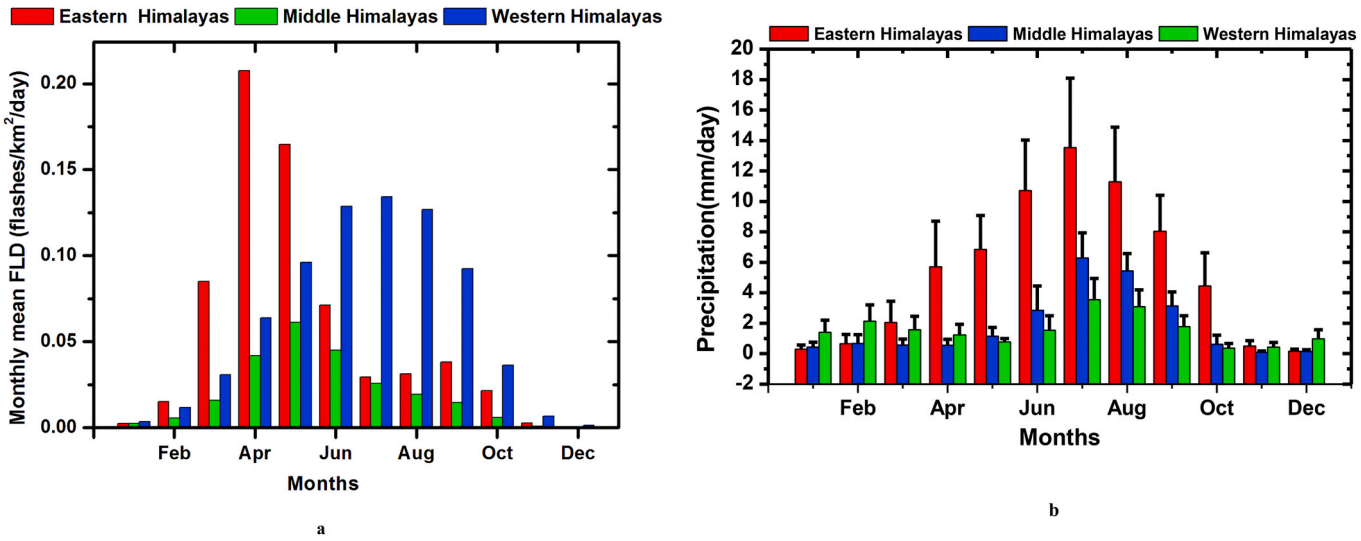

Fig. 2. a: Seasonal variation of monthly mean lightning flash density (LFD) over the Eastern, Middle and Western Himalayas from 1998 to 2013. **b: Seasonal** variation of monthly precipitation over Eastern, Middle and Western Himalayas.

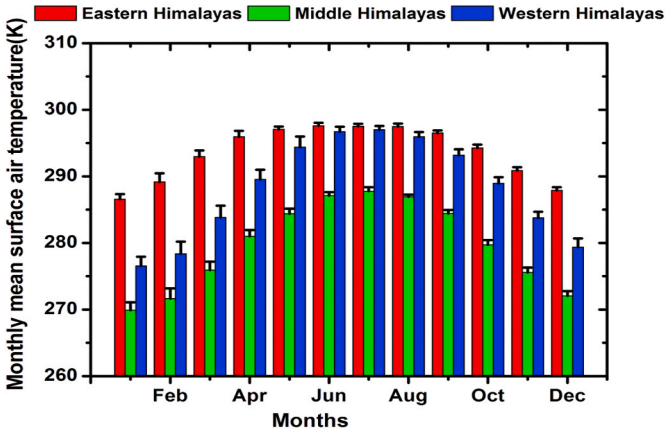

Fig. 3. Average monthly variation of Surface Air Temperature (SAT) in the Eastern, Middle and Western Himalayas from 1998 to 2012.

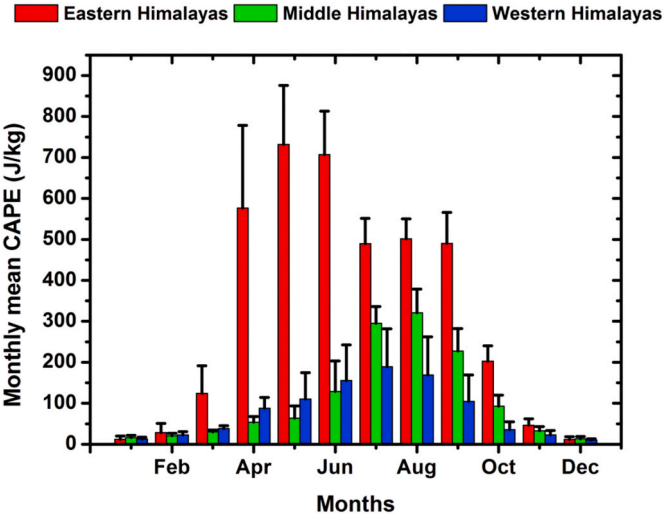

Fig. 4. Average monthly variation of Convective Available Potential Energy (CAPE) in the Eastern, Middle and Western Himalayas from 1998 to 2012.

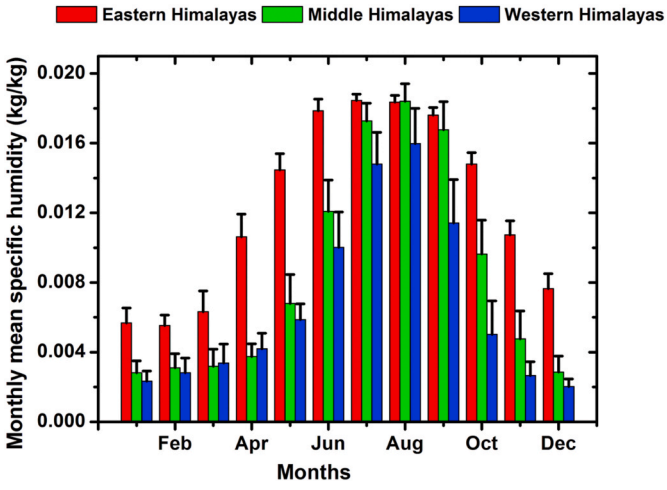

Fig. 5. Average monthly variation of Specific Humidity (SH) at 950 hPa in the Eastern, Middle and Western Himalayas from 1998 to 2012.

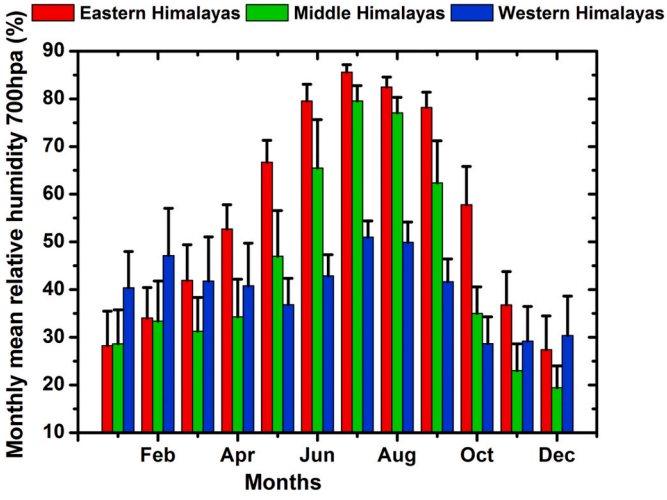

Fig. 6. Average monthly variation of Relative Humidity (RH) in the Eastern, Middle and Western Himalayas from 1998 to 2012.

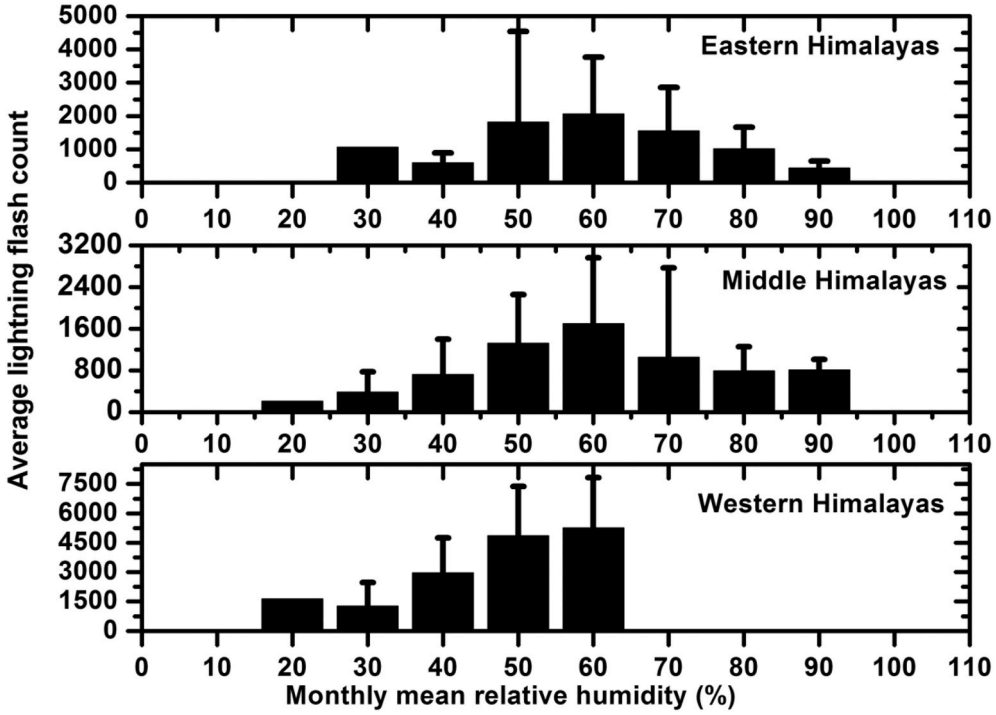

Fig. 7. Frequency distribution of LFC with respect to the RH (at 700 hpa) in the Eastern, Middle and Western Himalayas from 1998 to 2012.

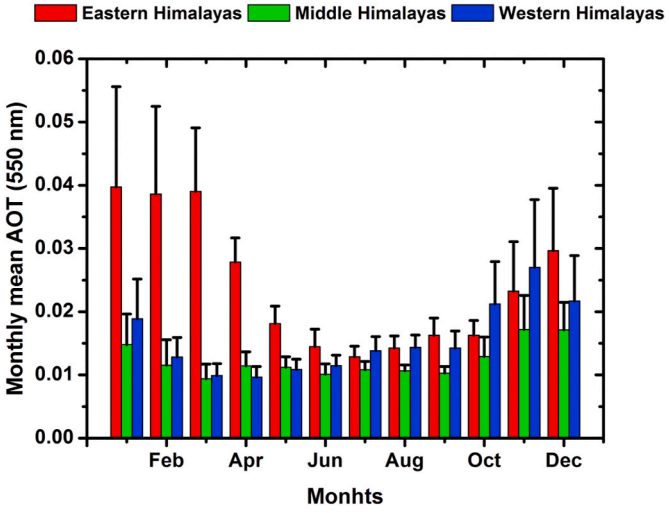

Fig. 8. Average monthly variation of Aerosol Optical Thickness (AOT) at 550 nm in the Eastern, Middle and Western Himalayas from 1998 to 2012.

parameters on LFD orbital track flashes are used. The analysis is performed in two steps. Monthly variation of all meteorological parameters over selected region is plotted and the correlation of meteorological parameters on LFD is calculated through scatter plot. The role of moisture on the inconsistent dependency of LFD on meteorological parameters (especially on CAPE and SAT) over the Himalayas is examined. Finally, range of the most favorable RH for the Himalayas lightning activity is estimated. However, spatial resolution is not constant for all meteorological parameters, the entire Himalayas region's spatial extent is concerned.

4. Results

We introduce a comparative analysis of LFD over the three Himalayan regions in Fig. 2a. In the Eastern Himalayas, the variation of LFD is a semiannual character. The maximum LFD occurs during the pre-monsoon, followed by the second enhancing tendency during the post-monsoon. The primary maxima of LFD during pre-monsoon occur in April. During the post-monsoon, a secondary peak in LFD appears in September.

Over the middle Himalayas, a single peak annual distribution is observed. A progressive decrement follows a gradual increment of LFD from January to May up to December. Higher LFD is found from April to June with maxima during May, followed by the second and third highest LFD during June and April.

Over the western parts of the Himalayas, a single peak annual distribution is observed. The variation of LFD over the Western Himalayas shows a different pattern than the Eastern and the Middle Himalayas. The LFD over the Western Himalayas is associated with the southwest monsoon from June to September (Jeelani et al., 2017). LFD increases from January and becomes maximum during July and decreases afterward. Instead of a distinct peak of LFD in July, we observe marginally similar higher LFD over Western Himalayas during August and June.

The seasonal variation of monthly precipitation over the Eastern, Middle, and Western Himalayas is shown in Fig. 2b. The precipitation pattern over the three regions is similar and shows prime maxima during July. Over the Eastern Himalayas, significant precipitation is observed from April to October. But, over the middle and western Himalayas, considerable rainfall is observed from June to September. Compared to the western Himalayas, relatively less precipitation is observed over the middle and western Himalayas all over the year.

To understand the role of associated meteorological parameters that drive the LFD variations over the three Himalayan regions, we have performed further analyses of a few essential parameters. We show the monthly change of SAT and CAPE in Fig. 3 and Fig. 4. Fig. 3 illustrated a similar trend over all the three Himalayan regions with higher values during June and July. The Eastern Himalayan region has a relatively higher SAT, followed by the Western Himalayas, and the least SAT is observed over the Middle Himalayas. The SAT analysis further reveals that the dynamic range of average SAT over the Eastern Himalayas is significantly less; the difference between winter and Summer SAT is only

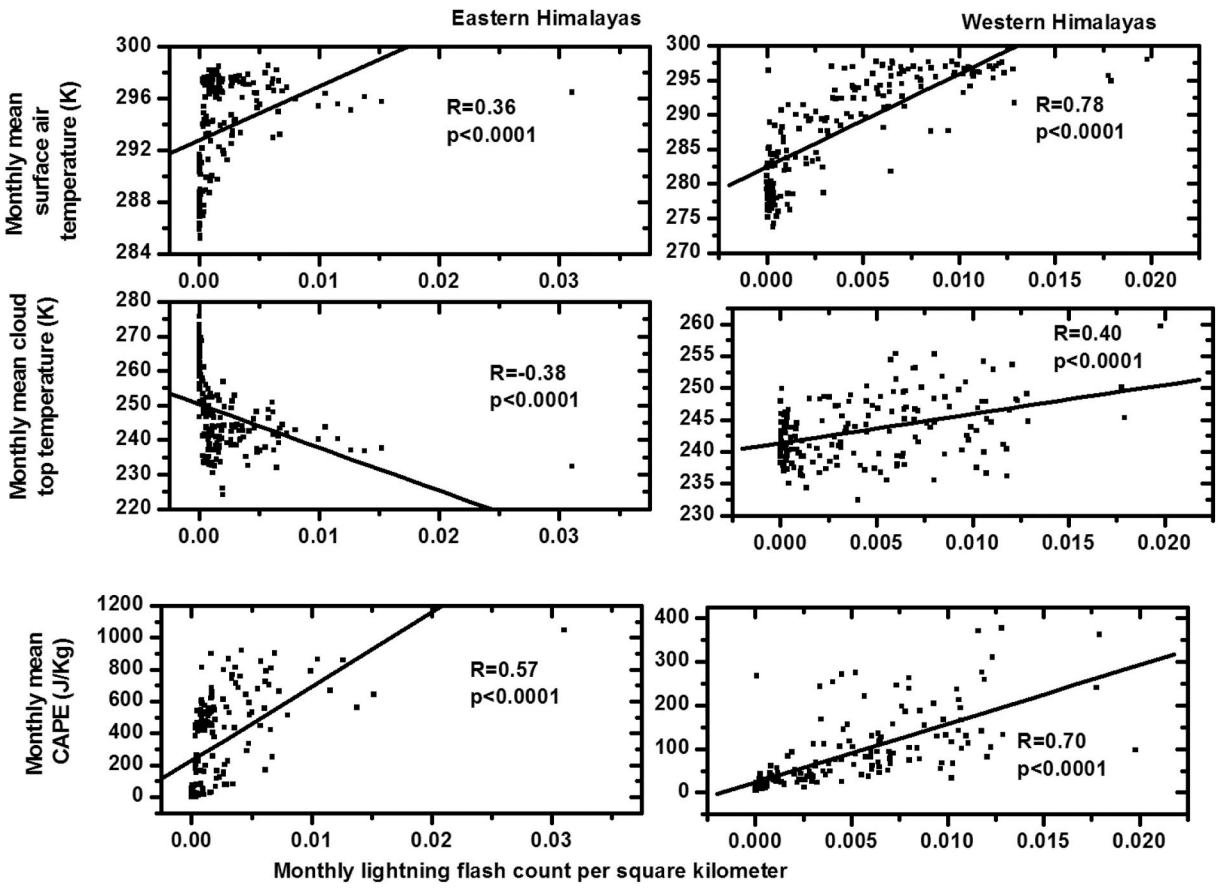

Fig. 9. Scatter plot of the monthly lightning flash density (LFD) with different meteorological parameters (CTT, CAPE, and SAT) for the Eastern and Western Himalayas. Values of correlation coefficients and the significance levels of the parameters are also shown in each plot.

around 10 K, whereas, for Middle and Western Himalayas, the difference is approximately 20 K. That explains the average SAT variability is comparatively higher over Middle and Western Himalayas than the Himalayas' Eastern part. It is also noticeable that an LFD over Eastern and Middle Himalayas is not associated with the highest SAT. Still, the LFD over Western Himalayas is related to the peak value of the SAT. But it is clear from Fig. 3 that the average SAT during April and May over the Eastern Himalayan region is very close to the peak SAT during June and July.

The difference is much perceptible for the other two Himalayan areas. The CAPE analysis in Fig. 4 shows the area-averaged monthly mean CAPE over Eastern Himalayas is predominately higher (11.4 J/kg to 731.8 J/kg) than the Middle Himalayas (13.2 J/kg to 320.9 J/kg) and western Himalayas (9.7 J/kg to 189.2 J/kg). The peak over the Eastern Himalayas occurs during May, whereas we observe a peak CAPE over the Middle and Western Himalayas during August and July. But the variation indicates a notion of predominantly higher CAPE during April and May, which is associated with the higher LFD over the Eastern Himalayas. The lower CAPE during March and the higher LFD over Eastern the Himalayas may be explained based on the other analysis of other meteorological parameters. But the variation of average CAPE supports the higher LFD during April and May over the Eastern Himalayas. We note the most convincing agreement between CAPE and LFD over the Western Himalayas. Peak LFD associated month coincides with the highest CAPE associated month as well. The higher LFD over the Middle Himalayan region during pre-monsoon is challenging to explain concerning the SAT and CAPE only. In addition to SAT and CAPE, other meteorological parameters might play a role in the generation of lightning.

The amount of atmospheric moisture, i.e., the amount of water vapor in the atmosphere, is measured in specific humidity (SH) and analyzed in Fig. 5 over the study region for the entire period. Among all the three Himalayan regions, the Eastern Himalayan region is more humid, followed by the Middle and Western Himalayas. The maximum SH over all the three Himalayan areas occurs during July–August only. This is associated with the Asian summer monsoon, which occurs first over the southeastern Bay of Bengal and southeastern Indochina peninsula in early May and covers the entire Southeast by the end of May (Zhang et al., 2004). In Nepal, 80% of the annual precipitation falls between June and September (Nayava, 1974). But a part of the monsoonal flow through the Bay of Bengal enters the North-Eastern part of India first. After obstructing the Eastern part of the Himalayas, the circulation turns toward the Middle Himalayas and goes further towards the Western Himalayan region. Therefore, the peak SH over the Eastern Himalayas during July, the same scale for the remaining two Himalayan areas, occurs during August. The presence of abundant moisture may reduce the SAT and CAPE's influence on the electrification that might further reduce the lightning activity. Therefore, to determine the quantitative measurement of the effective range of water vapor contributing to the maximum lightning activity, we have performed further analysis on the average relative humidity (RH) frequency distribution variation corresponding to the higher LFD. We show the results in Fig. 6 and Fig. 7.

Fig. 6 illustrates the atmospheric moisture content at 700 hPa concerning its saturation level and dew point relative to relative humidity. The pattern of RH variation at 700 hPa is similar to SH at 950 hPa. The peak RH is associated with the Monsoonal circulation. Due to the large water body SH, the RH is also highest over the Eastern Himalayas, followed by the Middle and Western Himalayas. This relation is not observed during January, February, and December due to less temperature over the Middle and Western Himalayas.

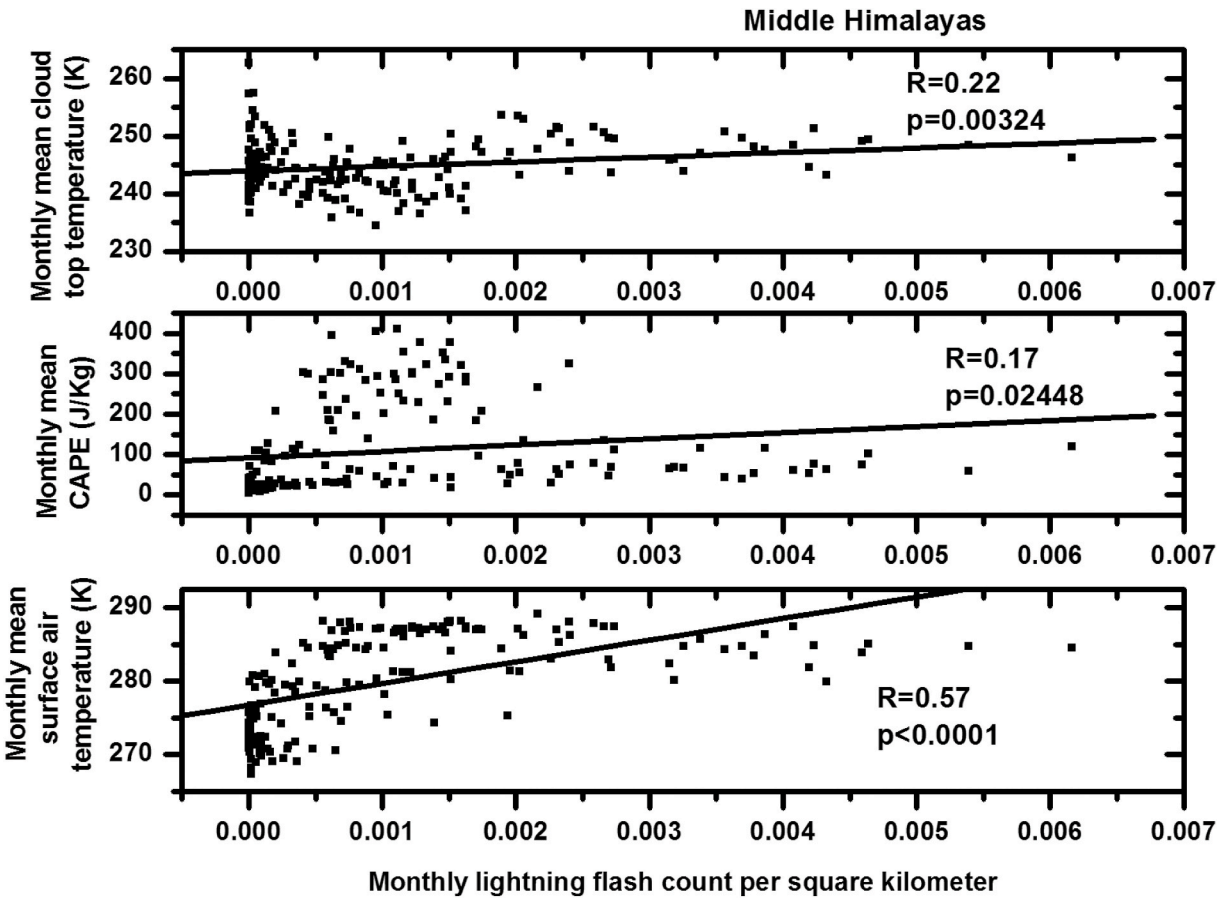

Fig. 10. Scattered plot of the monthly lightning flash density (LFD) with different meteorological parameters (CTT, CAPE, and SAT) for the Middle Himalayas. Values of correlation coefficients and the significance levels of the parameters are also shown in each plot.

The atmospheric water vapor availability is comparatively less over the Western Himalayas than the other two regions of interest. A higher average SAT with less moisture decreases the RH by increasing the water vapor's associated saturation level. As a result, due to the high saturation value and low moisture content, the RH over the Western Himalayan region is comparatively less than the remaining two areas of the Himalayas. The atmospheric water vapor increases the RH over the Eastern and the Middle Himalayas to 80% during monsoonal months. We show the distribution of LFD for the RH over all the three Himalayan areas in Fig. 7.

We computed the average LFD at different RH range, i.e., 0%–10%, 10%–20% etc. Overall, the most interesting observation is that the three Himalayan regions, the maximum LFD, are associated with the 50–60% RH at 700 hPa pressure level. We note that the lightning is well distributed over all the Eastern and Middle Himalayan regions over all the RH ranges with a peak around 50–60% RH range. But the distribution of lightning over the Western Himalayas is one-sided, and starting from 20% goes up to 60%. The bottom section of Fig. 7 shows an LFD above the RH value of 60% over the western Himalayan region. The value of RH over the western Himalayan region does not rise above 60%. It indicates less moisture content over the Western Himalaya that restricts RH value to lie within 60% even during the Monsoon season.

We investigated whether the atmospheric aerosol particle plays any crucial role in the lightning climatology over different Himalayan regions. In this respect, we have analyzed the monthly average Aerosol Optical Thickness (AOT) for all three Himalayan areas. We show the result in Fig. 8. The concentration of aerosol particles in the Himalayan region is higher in the winter seasons. We observe the next highest AOT during the pre-monsoon season over the Eastern and the Middle Himalayas. In contrast, monsoon and post-monsoon being the second-highest AOT associated season for the Western Himalayas. Interestingly that season is also associated with the highest LFD over the Eastern Middle and Western Himalayan region. One question may arise why peak AOT month is not associated with the peak LFD associated month. In this respect, we note that the monthly analysis of the Himalayas may not associate with the lightning activity. It is since the pre-monsoon and monsoonal precipitation may reduce the AOT.

In the analysis, zero-flashes are also considered. Dispersion in the meteorological variables for zero and close to zero flashes has been observed. We did not find the cut-off value of any meteorological variable for lightning activity. It is because lightning activity can be affected by many meteorological variables at a time. To understand the dependency of the LFD on the various meteorological parameters, we prepared a scatter plot between those parameters and LFD. We also computed the Pearson's correlation coefficient. We show the results in Figs. 9 and 10. SAT is well correlated ($R = 0.78$, $P < 0.0001$) with LFD in the Western Himalayas, moderately correlated ($R = 0.57$, $P < 0.0001$) in the Middle Himalayas, and poorly ($R = 0.36$, $p < 0.0001$) in the Eastern Himalayas. The correlation coefficient between CAPE and LFD is higher over the Western Himalayas ($R = 0.70$, $P < 0.0001$) than that of Eastern Himalayas ($R = 0.57$, $P < 0.0001$), whereas it is reduced ($R = 0.17$, $P = 0.02448$) in the Middle Himalayas. As seen from Figs. 9 and 10, the correlation between the CTT and LFD over the eastern region is negative ($R = -0.38$, $P < 0.001$), meaning they are inversely related. In contrast, LFD and CTT over the western Himalayas are moderately correlated ($R = 0.40$, $P < 0.0001$), and that over the middle Himalayas are poorly correlated ($R = 0.22$, $P = 0.00324$).

The correlation analysis of all parameters shows fair agreements over the Western Himalayas than the other two regions. It signifies that the Eastern and the Middle Himalayas' lightning climatology have different

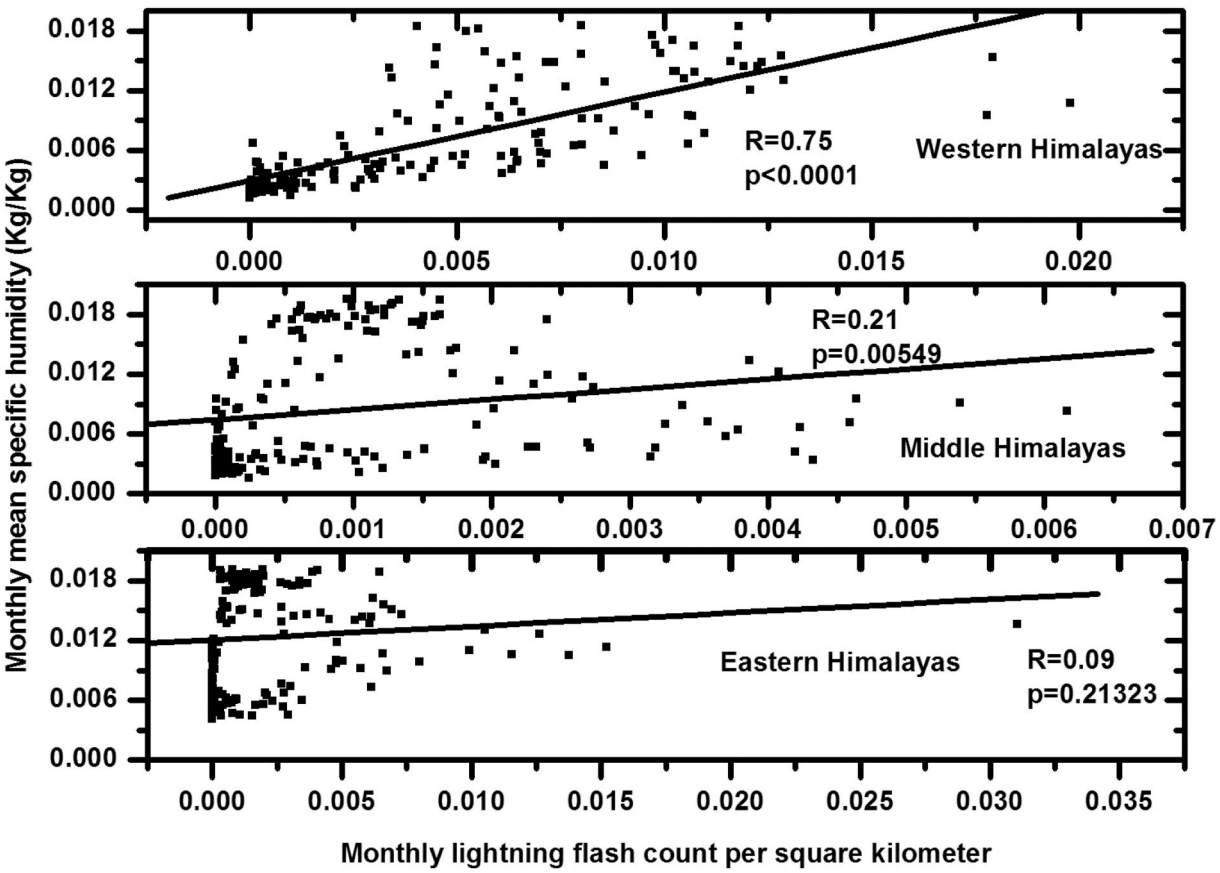

Fig. 11. Scattered plot of the monthly lightning flash density (LFD) with specific humidity in the different Himalayan regions. Values of correlation coefficients and the significance levels of the parameters are also shown in each plot.

characteristics than the Western part of the Himalayas. The possible reasons could be (i) the complex combination of a higher abundance of water vapor, (ii) aerosol loading, (iii) terrain height difference, (iv) the difference in vegetation index. The most humid region has a negative correlation with the CTT. It could be due to the presence of abundant moisture above the cloud base, whereas the dry area has a positive relationship with CTT due to the opposite effect. Higher CAPE with suitable relative humidity in the monsoon shows a good correlation with lightning activity.

We illustrate SH and LFD for the three different regions of the Himalayan belt in Fig. 11. The LFD has an insignificant correlation ($R = 0.09$, $P = 0.21323$) over the Eastern Himalayas, and the correlation increases over the Middle Himalayas ($R = 0.21$, $P = 0.00549$) and the Western Himalayas ($R = 0.75$, $P < 0.001$), respectively. It shows the correlation coefficient between SH and LFD increases in the less moist region. The dependency of LFD on precipitation and wind speed is shown in Fig. 12. Precipitation is positively correlated with LFD ($R = 0.21$, $P = 0.00549$ over the Eastern Himalayas, $R = 0.23$, $P = 0.00206$ over the Middle Himalayas, and $R = 0.49$, $P < 0.0001$ over the Western Himalayas). But, the correlation between LFD and wind speed is negative overall Himalayas.

5. Discussion

The Himalayan region is characterized by topographic heterogeneity and land-use variability with a significant variation in regional climate patterns. NDVI index over the Eastern Himalayas is higher, followed by the Western Himalayas, and the Middle Himalayas has the least NDVI index. The Middle Himalayas cover higher mountains, followed by the Western Himalayas. LFD is closely associated with the low land area and hilly regions than higher Mountains. In the western part of the Himalayan belt, almost one-third of annual precipitation occurs during the winter due to western disturbance (Dimri et al., 2013). During May and June, the moisture during the monsoon comes from the Bay of Bengal in the North-East region. For the North-West region, the humidity comes in June and July (Penki and Kamra, 2013). When the moist air mass from the Bay of Bengal enters the land region, the thermal heating and topography enhance moisture's uplifting and leads the thunderstorms. The high mountains of the Himalayas generate strong updrafts necessary for the deep convective events through their interaction with the prevailing winds (Murugavel et al., 2014).

The Eastern Himalayan region is warmer, moist, and with relatively higher Precip, CAPE, SAT, SH, RH (except January, February, and December), and AOT. The most increased lightning activity is during pre-monsoon and followed by post-monsoon. Precip, SAT, CAPE, and SH influenced positively over this region and showed a positive correlation, but CTT affected negatively and shown a negative correlation. More LFD is observed during 50–60% RH. Middle Himalayas lightning activity is influenced by low SAT and CAPE, moderate SH, RH, AOT, and precipitation. The lightning activity is annual, with a single peak during May. CAPE, SAT, CTT, Precip, CTT, and SH show a positive correlation over this region. More lightning activity is followed by 50–60% RH. The Western Himalayas lightning activity is annual, with a prime peak during July. Moderate SAT and AOT, low precipitation, CAPE, SH, and RH (except January, February, and December) affect lightning activity. The correlation of LFD with Precip, CAPE, SAT, SH, and CTT is positive. Higher LFD is in the range of 50–60% RH. The density plot (Fig. 1b) reveals that the lightning activity is active all months except December (nominal value). The high lightning activity starts from March over the Eastern Himalayas and spreads throughout the Himalayas in May.

The Eastern Himalayan region is generally warmer and humid than the other two Himalayan regions. The Middle Himalayan region has a

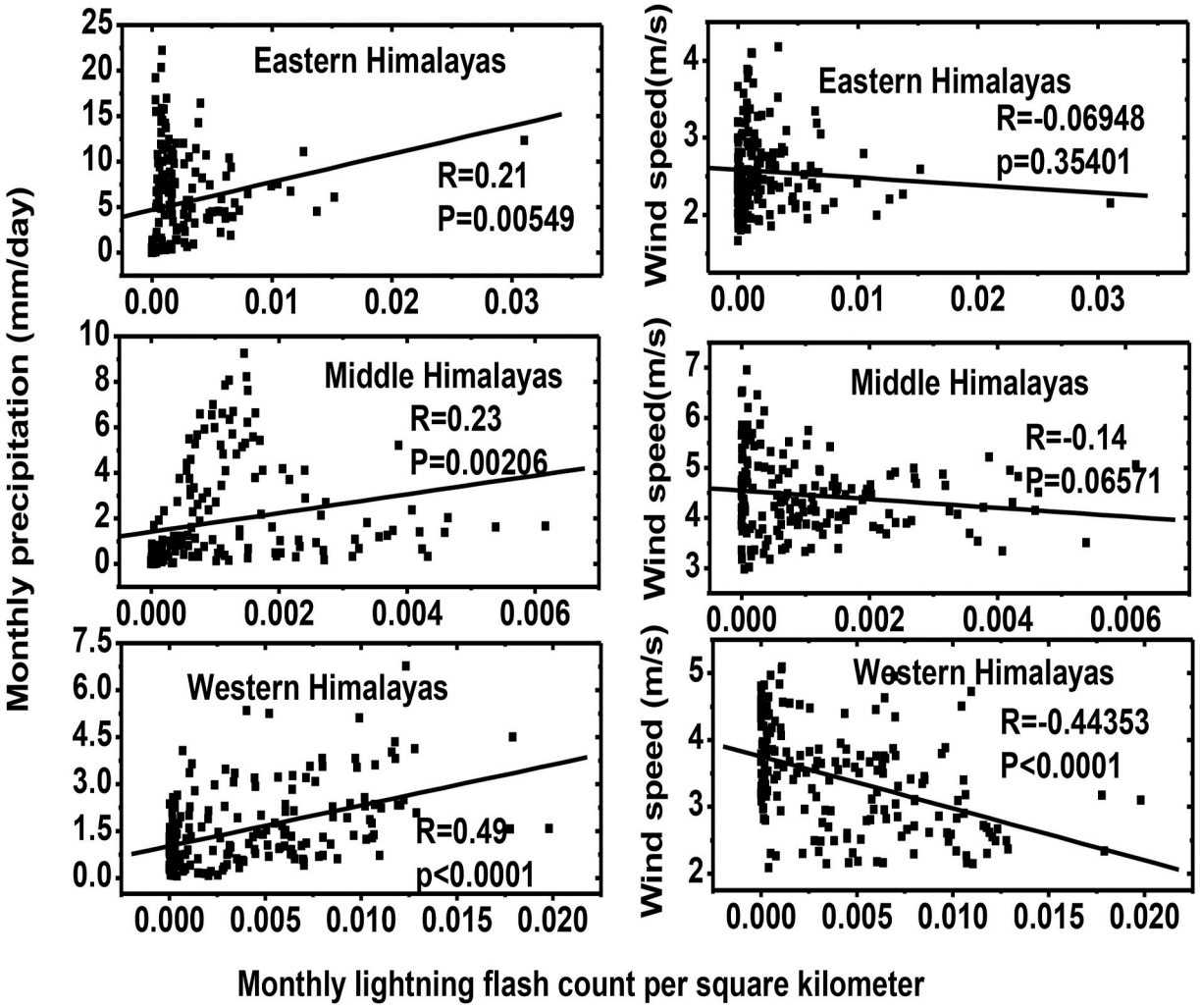

Fig. 12. Scatter plot of monthly mean lightning flash density (LFD) with monthly mean precipitation and surface wind speed in different Himalayan region. Values of correlation coefficient and the significance levels of the parameters are also shown in each plot.

minimum temperature as the selected study region covers mountains and slopes with higher altitudes than the other areas. The low land southern part of the Middle Himalayan region is relatively warmer than the northern part. Over this region, the thermodynamic instability generated at high temperate flat land produces lightning over the plains, hills, and sparsely mountains. The Western Himalayan region has nonuniform atmospheric convection. It covers the warmer part of Pakistan, Afghanistan, India, and some parts of the mountain's region. The annual variation (variation from January to December) of the SAT over the Western Himalayan region is significantly higher than the Middle Himalayas. Besides, fewer amounts of water bodies and atmospheric water vapor make this region very hot and dry.

On the contrary, the abundance of water bodies in BOB's close vicinity, the moisture content over the Eastern Himalayas, is significantly higher than the other two Himalayan regions. An increase in surface temperature after the winter season increases the atmosphere's moisture-holding capacity and holds more moisture. As the surface heats up and reaches a temperature around 290–293 K, sufficient CAPE builds up so that the available water vapor (a measure of specific humidity) coincides with pre-monsoon and monsoon and can enter the mixed-phase region of the thunderstorm to produce enhanced electrical activity (evident from Fig. 4). The enhanced water vapor with sufficient SAT and CAPE may be critical elements to increase the Eastern region's lightning activity in April and May. This phenomenon is evident in the analysis. Also, the thunderstorm and distinct squall lines sometimes advert from the northwestern and south-eastern side of India that is ultimately dissipated over the eastern part of the Himalayas, resulting in a significant amount of lightning precipitation. Over the western region, water vapor becomes accessible after the monsoon season. At that point, the temperature likewise becomes favorable (over 290 K) for the generation of adequate CAPE, resulting in enhanced activity in LFD.

The observed dependence of LFD on SAT and CAPE during the analysis over the different parts of the Himalayas is consistent with the previous results observed in various parts of the globe (Siingh et al., 2014; Pinto and Pinto 2008; Zheng et al., 2016). As the surface warms up, the evaporation rate increases moisture in the atmosphere, which is the crucial element of the global water cycle (Huntington, 2005). Sufficient SAT and CAPE uplift the humidity to the higher part of the atmosphere through the convection mechanism. As the moist air rises, it cools down. When the moisture in the atmosphere uplifts, some water vapor in the rising air condenses, and puffy cumulus clouds may form in the atmosphere. As the cumulus cloud continues to grow, the tiny water droplets within the cloud combine and become more abundant. The possibility of the formation of drops and updrafts within it increases as the moisture in the atmosphere increases. The precipitation may grow at a low height if the relative humidity is relatively higher. We observe this phenomenon above sea or water bodies with a higher-level relative humidity. The base of the cloud over land and sea is illustrated by Warren et al. (2007). Suppose the moisture reaches sufficient height for saturation and the humidity above the cloud is relatively high. In that

case, the corresponding downdraft and updraft of water with ice crystal may electrify the cloud and form thunder and lightning.

Suitable moisture with sufficient CAPE and SAT during pre-monsoon in the Eastern and the Middle Himalayas and during the monsoon over the Western Himalayas is the primary cause of lightning activity. Greater CAPE and SAT may not yield more lightning if moisture saturates before reaching the mixed-phase region. So, LFD has a better correlation with CAPE and SAT in the moderately moist area.

The surface characteristics affect the dry stage of conditional instability and, ultimately, updraft strength of the moist air. It is the primary factor for cloud electrification. Conditional instability is a two-stage process, a dry stage in the planetary boundary and a wet stage above the cloud base. As the relative humidity drops, the dry thermal buoyancy increases, which ultimately increases the cloud base height, but the accessibility of adequate moisture to create a thunderstorm is an essential factor for cloud electrification and lightning. If RH is significantly less, the cloud base height is so high that cloud formation is prohibited entirely. Such low RH associated with high cloud formation is noticeable over the deserts (Williams and Stanfill, 2002). A rapid increase in moisture with a little temperature rise may reach the atmosphere's saturation level, which hinders further increase in the water's height and decreases the formation of thunderstorm and lightning activity. We observe this phenomenon in the monsoon season over the Eastern and Middle Himalayas. The amount of aerosol is responsible for surface warming. The temperature rise may increase in CAPE value and enhance the lightning activity transporting the aerosols to the mixed-phase region as the secondary effect.

Over Eastern Himalayas, higher temperate and moisture, enough CAPE, and SAT with moderate RH (50–60%) in pre-monsoon increases the cloud's height, resulting in more lightning flashes. Conversely, the least moisture with average RH (<50%) from October to March reaches the dew point on increasing the altitude. Still, the CAPE and SAT are insufficient to create adequate updraft and downdraft, a necessity for cloud electrification. Besides, the least moisture during this period similarly supports the atmospheric stability. Therefore, increasing the cloud height (lowering CTT) does not respond positively to electrification over the Middle and Western Himalayas. Consequently, the opposite effect of LFD with CTT is observed.

6. Concluding remarks

The lightning density over the Himalayan belt has significant heterogeneity. Higher lightning density in the Western Himalayas than the Eastern Himalayas is perceived during monsoon and post-monsoon, whereas a reverse phenomenon is observed during pre-monsoon. The Middle Himalayas is the least lightning zone among the three. The derived dependency of LFD on several meteorological parameters (i.e., CAPE, SAT, RH, and SH) in terms of the correlation coefficient shows that LFD positively correlates with SAT in the Western Himalayas, moderately in the Middle Himalayas, and least in the Eastern Himalayas. The correlation of LFD with CAPE is significant in the Western Himalayas, moderate for the Eastern Himalayas but insignificant in the Middle Himalayas. Higher moisture during monsoon and post-monsoon and insufficient CAPE and SAT during winter feed seasonal lightning (i.e.in pre-monsoon seasons) over in the Eastern Himalayas. Moderate humidity from March to September, mainly sufficient moisture during the monsoon seasons, feed the annual lightning with peak activity during monsoon over the Western Himalayas. The comparatively low temperature and humidity play an important role in less lightning activity over the Middle Himalayas. The driven instability created by SAT and CAPE is sensitive to lightning; however, the relative humidity at 700hpa is very crucial, and 50–60% is most favorable for the cloud electrification and lightning activity over the Himalayan region.

Declaration of competing interest

The authors declare that they have no known competing financial interests or personal relationships that could have appeared to influence the work reported in this paper.

Acknowledgments

The authors are thankful to the Global Hydrology and Climate Center Lightning Research Team at National Aeronautics and Space Administration (NASA) Marshall Space Flight Center for providing the Lightning Imaging Sensor (LIS) data and National Oceanic and Atmospheric Administration (NOAA) for providing Convective Available Potential Energy (CAPE) and NOAA-NCEI (National Centers for the Environmental Information) for topography data. We are also thankful to Goddard Earth Sciences Data and Information Systems for providing other meteorological parameters such as cloud top temperature (CTT), relative humidity (RH), and surface air temperature (SAT). NAM S&T Centre supports the work by providing research training fellowship for developing country scientists (RTF-DCS)–Award of Fellowship for 2016–17 to the first author of this manuscript. We express our thanks to LDN project fund from the Society for Applied Microwave Electronics Engineering & Research (SAMEER), Ministry of Communications & Information Technology, Government of India, DST-FIST fund reference Ref.SR/FST/PSI-191/2014, and University Grants Commission SAP fund reference F.530/23/DRS-I/2018(SAP-I), Government of India.

References

Boccippio, D.J., Koshak, W.J., Blakeslee, R.J., 2002. Performance assessment of the optical transient detector and lightning Imaging sensor. Part I: predicted diurnal variability. J. Atmos. Ocean. Technol. 19, 1318–1332.

Dimri, A.P., Yasunari, T., Wiltshire, A., Kumar, P., Mathison, C., Ridley, J., Jacob, D., 2013. Application of regional climate models to the Indian winter monsoon over the western Himalayas. Sci. Total Environ. 468–469, S36–S47.

Dewan, A., Ongee, E.T., Rafiuddin, M., Rahmin, M.M., Mahmood, R., 2018. Lightnig activity associated with precipitation and CAPE over Bangaladesh. Int. J. Climatol. 38 (4), 1649–1660.

Deierling, W., Petersen, W.A., 2008. Total lightning activity as in indicator of updraft characteristics. Journal of Geiphsical Research 113, D16210.

Guha, A., Banik, T., Roy, R., De, B.K., 2017. The effect of El Nino and La Nina on lightning activity: its relation with meteorological and cloud microphysical parameters. Nat. Hazards 85, 403–424.

Hobbs, P.V., Burrows, D.A., 1966. The electrification of an ice sphere moving through natural clouds. J. Atmos. Sci. 23, 757–763.

Huntington, T.G., 2005. Evidence of intensification of the global water cycle: review and analysis. J. Hydrol. 319, 83–95.

Jeelani, Ghulam, Deshpande, Rajendrakumar, Shah, Rouf, Hassan, Wasim, 2017. Influence of southwest monsoons in the kashmir valley, western Himalayas. Isot. Environ. Health Stud. 53, 1–13. https://doi.org/10.1080/10256016.2016.1273224.

Kandalgaonkar, S.S., Tinmakar, M.I.R., Kulkarni, J.R., Nath, A., Kulkarni, M.K., Trimbke, H.K., 2005. Spatio-temporal variability of lightning activity over Indian region. J. Geophys. Res. 110, D11108.

Makela, A., Sherstha, R., Karki, R., 2014. Thunderstorm characteristics in Nepal during the pre-monsoon season 2012. Atmos. Res. 137, 91–99.

Mazarakis, N., Kotroni, V., Lagouvardos, K., Argiriou, A.A., 2008. Storms and lightning activity in Greece during the warm periods of 2003-06. Journal of Applied meteorology and climatology 47, 3089–3098.

Ming, M.A., Shanchang, T.A.O., Zhu, Baoyou, Weitao, L.U., Tan, Yongbo, 2005. Response of global lightning activity to air temperature variation. Chin. Sci. Bull. 50 (22), 2640–2644.

Molinie, G., Jacobson, A.R., 2004. Cloud-to-ground lightning and cloud top brightness temperature over the contiguous United States. J. Geophys. Res. 109, D13106. https://doi.org/10.1029/2003JD003593.

Murugavel, P., Pawar, S.D., Gopalakrishan, V., 2014. Climatology of lightning over Indian region and its relationship with convective available potential energy. Int. J. Climatol. 34, 3179–3187.

Mattos, E.V., Machado, L.A.T., 2011. Cloud-to-ground lightning and mesoscale convective system. Atmos. Res. 99, 377–390.

Nath, A., Manohar, G.K., Dani, K.K., Devara, P.C.S., 2009. A study of lightning activity over land and oceanic region of India. Journal of Earth System Science 118 (5), 467–481.

Nayava, Janak, 1974. Heavy monsoon rainfall in Nepal. Weather 29, 443–450, 10.1002/j.1477-8696. 1974.tb03299.x.

Penki, R.K., Kamra, A.K., 2013. The lightning activity associated with the dry and moist convections in the Himalayan Regions. Journal of Geophysical Research Atmospheres 118, 6246–6258. https://doi.org/10.1002/jgrd.50499.

Pinto Jr., O., Pinto, I.R.C.A., 2008. On the sensitivity of cloud-to-ground lightning activity to surface air temperature changes at different timescales in São Paulo, Brazil. Journal of Geophysical Research Atmospherics 113, D20123. https://doi.org/10.1029/2008JD009841.

Qie, K., Tian, W., Wang, W., Wu, X., Yuan, T., Tian, H., Luo, R., Wang, T., 2020. Regional trend of lightning activity in the tropic and subtropics. Atmos. Res. 242, 104960.

Rakov, V.A., Uman, M.A., 2003. Lightning: Physics and Effects. Cambridge University, Cambridge, p. 687p. https://doi.org/10.1017/CBO9781107340886.006.

Reeve, N., Toumi, R., 1999. Lightning as an indicator of climate change. J.R. Meteorol. Soc 125, 893–903.

Saha, K, Damase, NP, Banik, T, Paul, B, Sharma, S, De, BK, Guha, A, 2019. Satellite-based observation of lightning climatology over Nepal. https://doi.org/10.1007/s12040-019-1239-x.

Saunders, C.P.R., Peck, S.L., 1998. Laboratory studies of the influence of the rime acceleration rate on charge transfer during crystal/graupel collisions. J. Geophys. Res. 103 (D12), 13949–13956.

Siingh, D., Buchunde, P.S., Singh, R.P., Nath, A., Kumar, S., Ghodpage, R.N., 2014. Lightning and convective rain study in different parts of India. Atmos. Res. 35–48.

Takahashi, T., 1978. Riming electrification as the charge generation mechanism in thunderstorms. J. Atmos. Sci. 35 (8), 1536–1548.

Tinmaker, M.I.R., Aslam, M.Y., Chate, D.M., 2015. Lightning activity and its association with rainfall and convective available potential energy over Maharashtra, India. Nat. Hazards 77, 293–304.

Warren, S.G., Eastman, R.M., Hahn, C.J., 2007. A survey of changes in cloud cover and cloud types over land from surface observations, 1971–96. J. Clim. 20, 717–738.

Williams, E.R., 1994. Global circuit response to seasonal variation in global surface air temperature. Mon. Weather Rev. 122 (8), 1917–1929.

Williams, E., Stanfill, S., 2002. The physical origin of land-ocean contrast in lightning activity. Compt. Rendus Phys. 3, 1277–1292.

Ya-Jun, X., Xiu-Shu, Q., Yun-Jun, Z., Tie, Y., Ting-long, Z., 2006. Regional responses of lightning activity to relative humidity of surface. Chin. J. Geophys. 49 (2), 311–318.

Zhang, Z., Chan, J.C.L., Ding, Y., 2004. Characteristics, evolution and mechanisms of the summer monsoon onset over Southeast Aaia. Int. J. Climatol. 24, 1461–1482.

Zheng, D., Zhang, Y., Meng, Q., Chen, L., Dan, J., 2016. Climatology of lightning activity in south China and its relationship to precipitation and convective available potential energy. Adv. Atmos. Sci. 33, 365–376.